

Supplementary Information

**Observation of nonvolatile magneto-thermal switching in
superconductors**

Hiroto Arima¹, Md. Riad Kasem¹, Hossein Sepehri-Amin², Fuyuki Ando²,

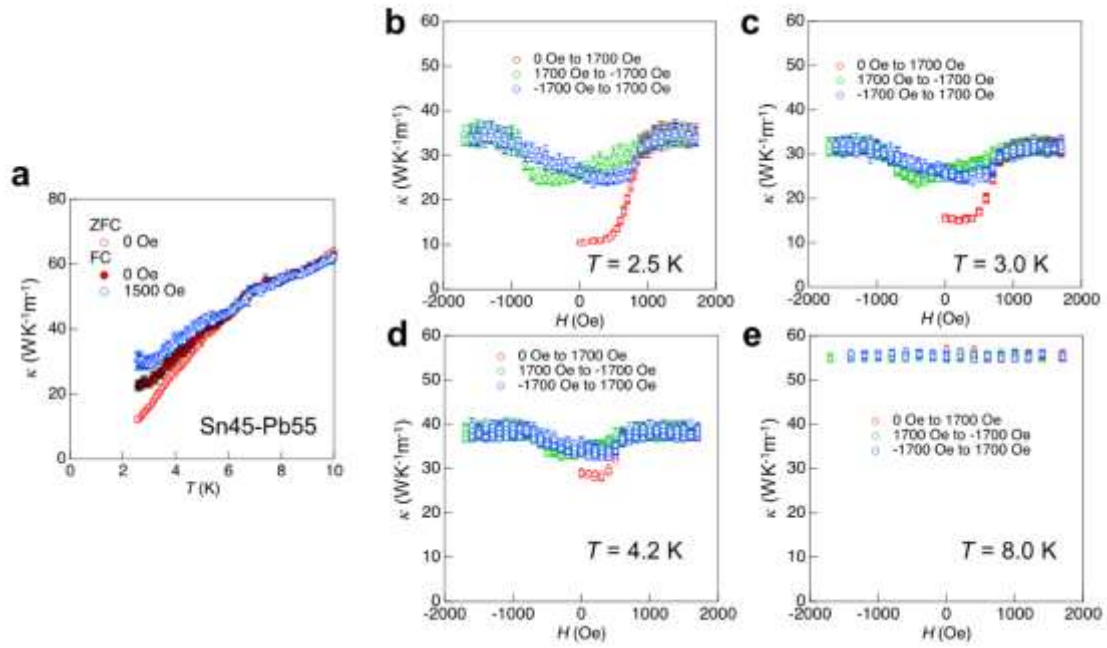
Ken-ichi Uchida², Yuto Kinoshita³, Masashi Tokunaga³, Yoshikazu Mizuguchi^{1*}

*¹Department of Physics, Tokyo Metropolitan University; 1-1, Minami-osawa, Hachioji,
192-0397, Japan.*

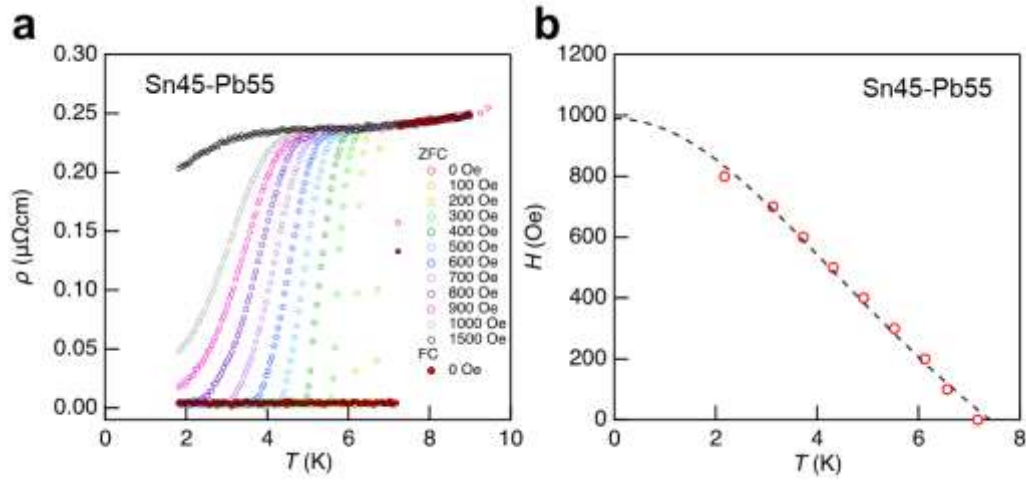
²National Institute for Materials Science; 1-2-1, Sengen, Tsukuba, 305-0047, Japan.

*³Institute for Solid State Physics, University of Tokyo, 5-1-5, Kashiwanoha, Kashiwa,
277-8581, Japan*

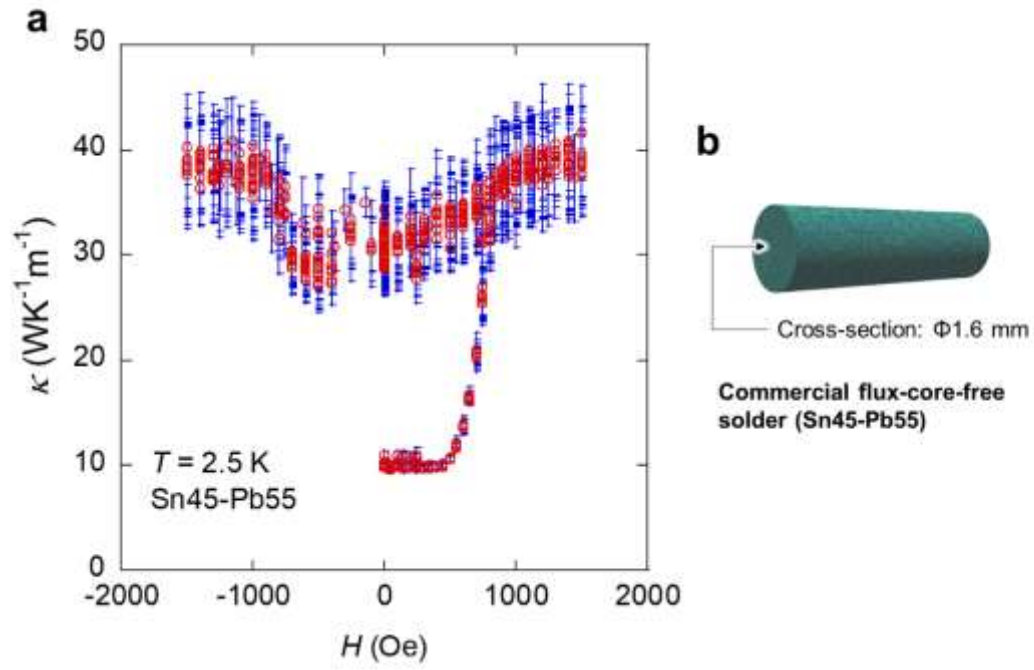
*Corresponding author: mizugu@tmu.ac.jp



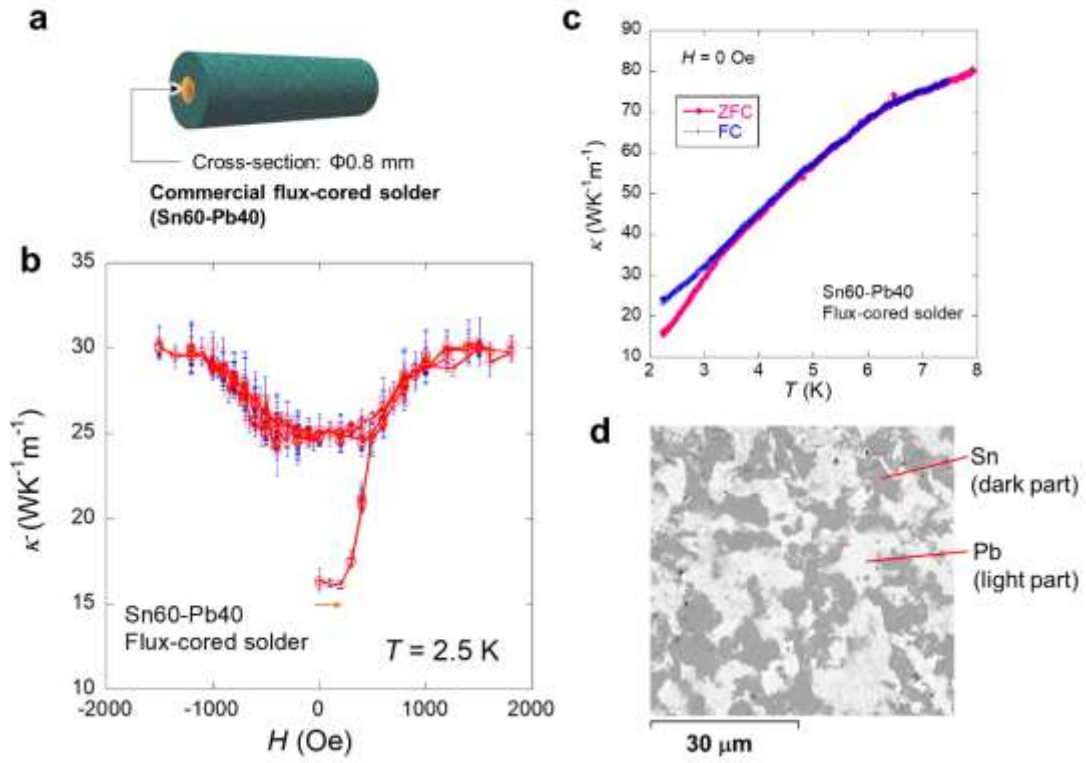
Supplementary Figure 1 | Measurement errors on nonvolatile magneto-thermal switching characteristics of the flux-core-free solder (Sn45-Pb55). **a**, Thermal conductivity-temperature (κ - T) plot for the flux-core-free Sn45-Pb55 solder (rectangular-shaped sample shown in the main text) with error bars (standard deviations). FC (0 Oe) means that the sample was field-cooled (FC) from 10 K to 2.5 K, and the data were taken after reducing the external field. **b–e**, κ - T plots taken at $T = 2.5, 3.0, 4.2$, and 8.0 K with error bars.



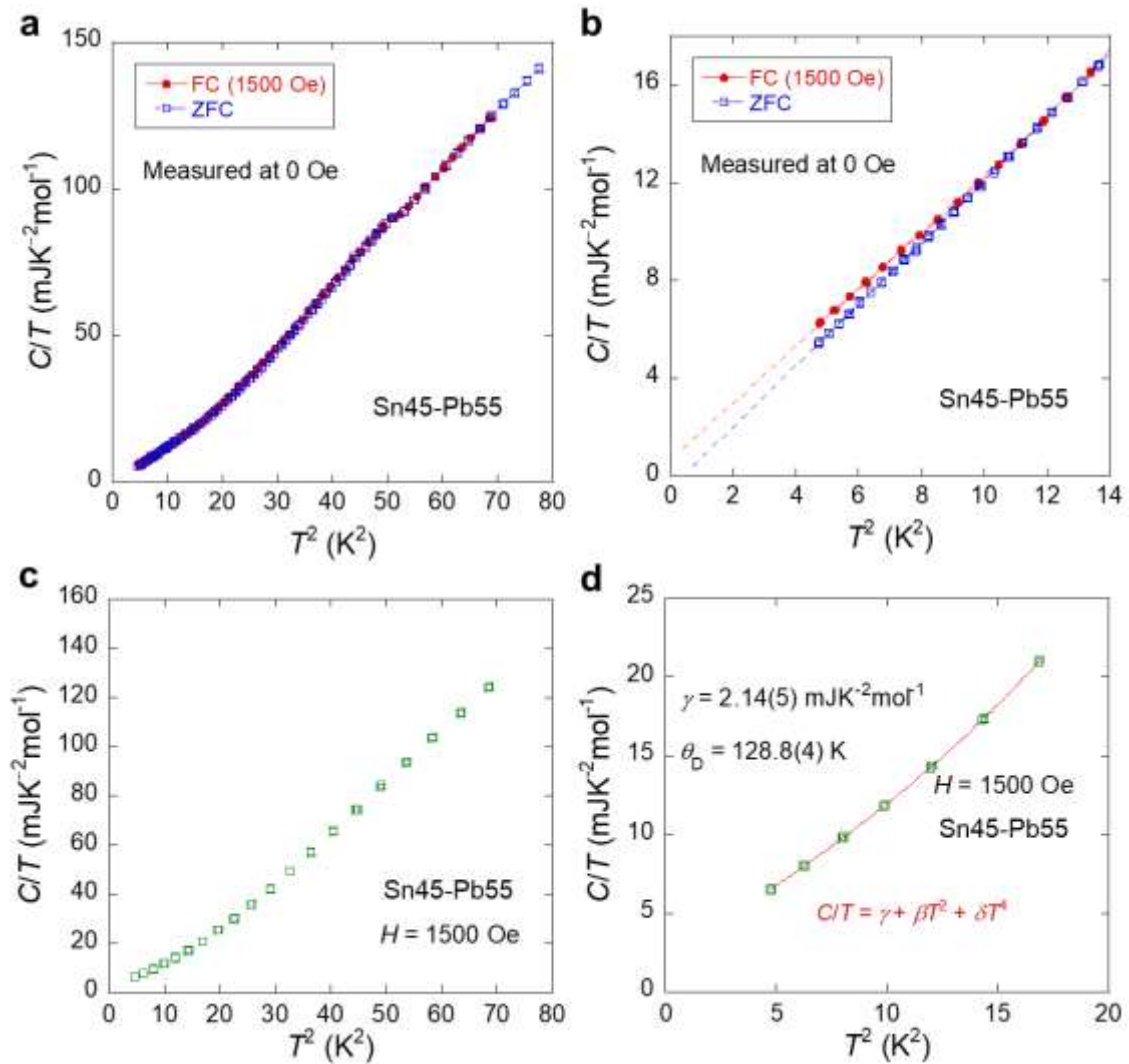
Supplementary Figure 2 | Transport properties of the flux-core-free solder (Sn45-Pb55). **a**, Temperature dependence of the electrical resistivity for the flux-core-free Sn45-Pb55 solder. The measurements were performed by heating the sample from the lowest temperature after ZFC and FC. For most cases, the sample was zero-field-cooled and magnetic fields in the legend are applied at the lowest temperature. For, FC data, the sample was field-cooled under 1500 Oe, and the field was reduced to zero at the lowest temperature before the measurement. **b**, H - T phase diagram estimated from the temperature dependence data.



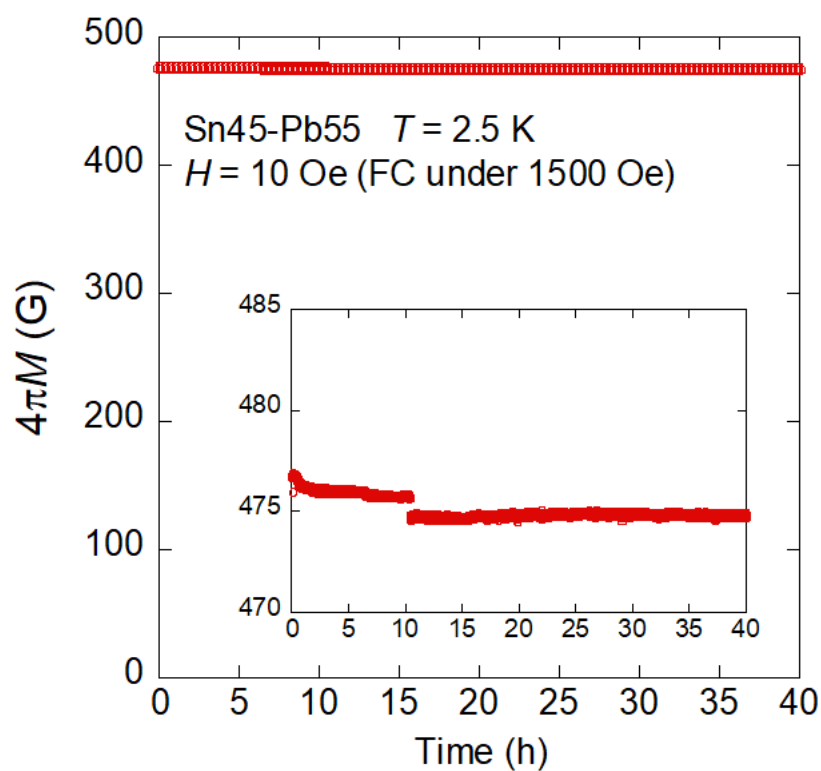
Supplementary Figure 3 | Nonvolatile MTS for wire-shaped Sn45-Pb55. **a**, κ - H plot for a $\phi 1.6 \text{ mm}$ wire of the flux-core-free Sn45-Pb55 sample (without polishing) taken at $T = 2.5 \text{ K}$. **b**, Schematic image of the measured solder sample.



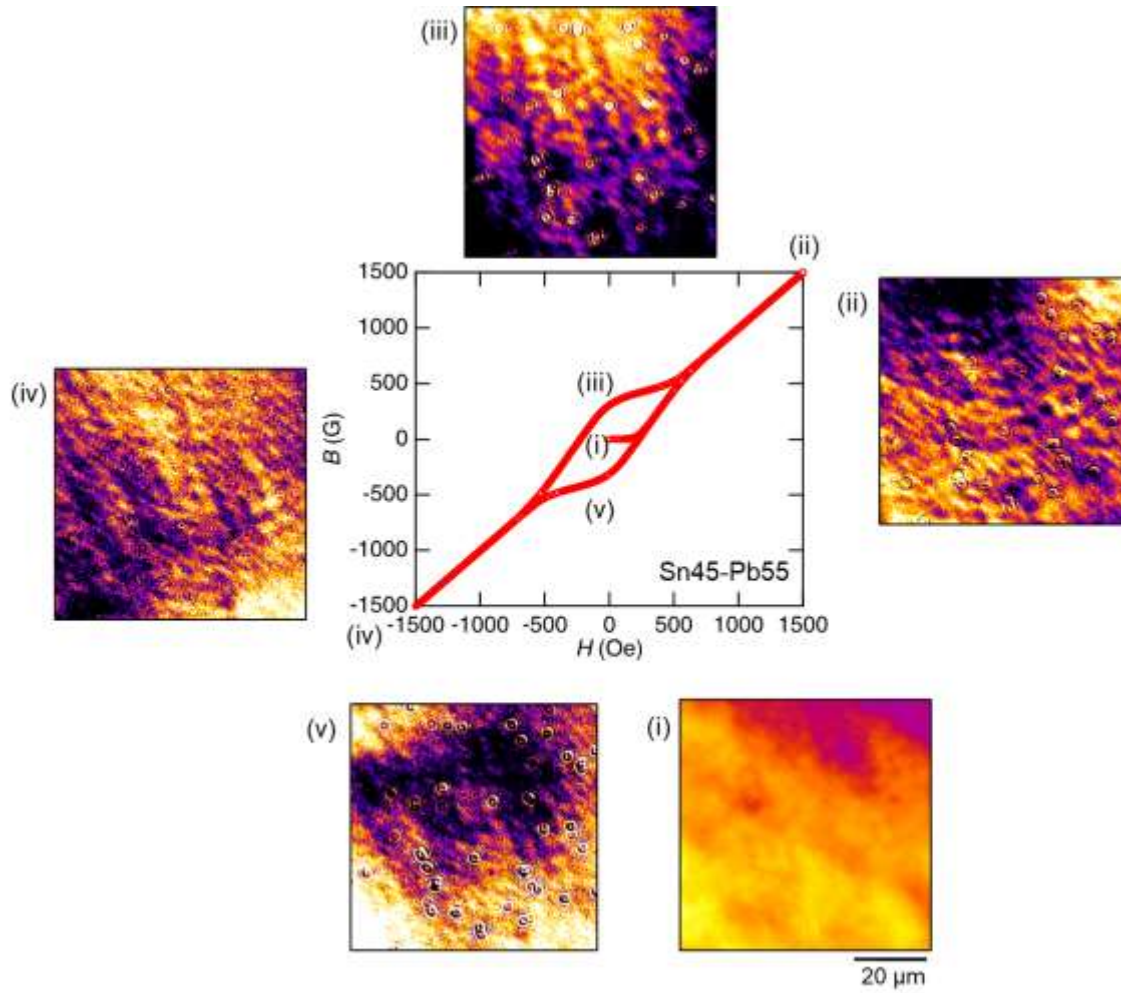
Supplementary Figure 4 | Nonvolatile MTS for the flux-cored solder. **a**, Schematic image of the measured solder sample. **b**, κ - H plot for a $\phi 0.8$ mm wire of the flux-cored Sn60-Pb40 sample (without polishing) taken at $T = 2.5$ K. **c**, T dependence of κ measured at $H = 0$ Oe after ZFC and FC (FC under $H = 1500$ Oe). **d**, Scanning electron microscope (SEM) back-scattering image.



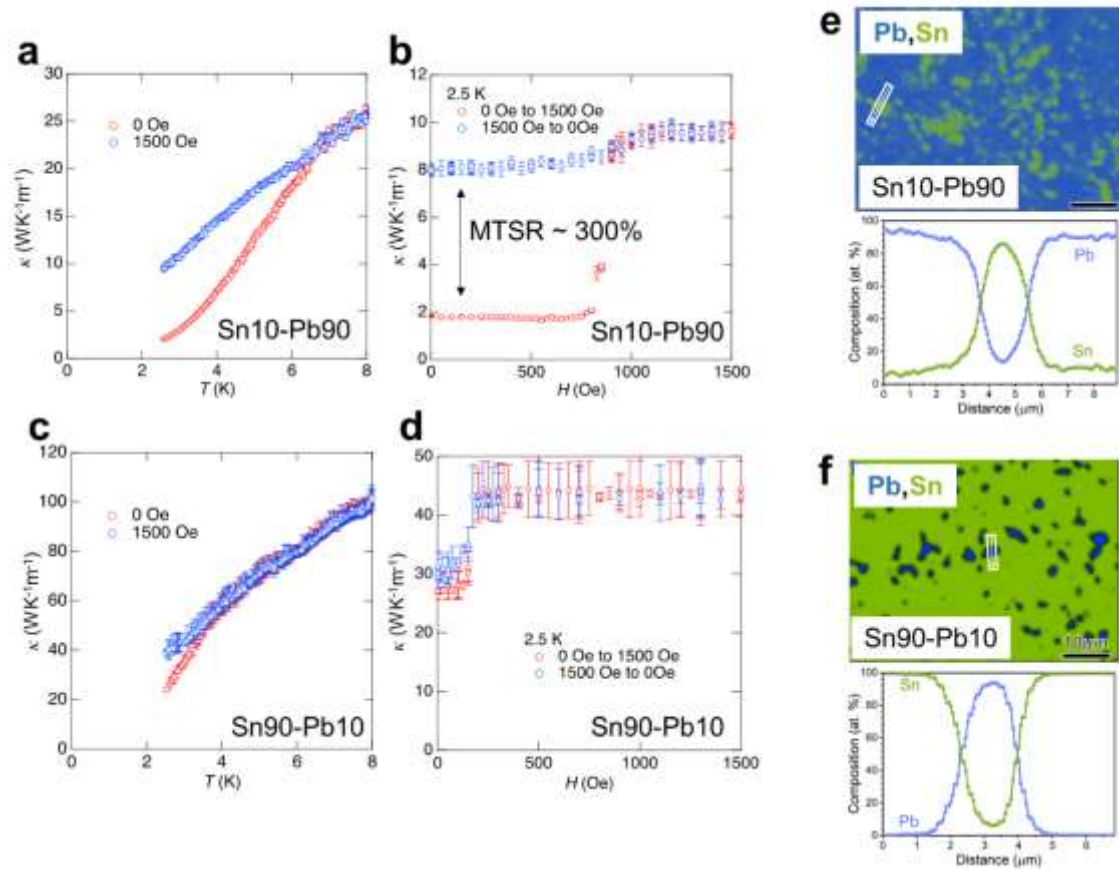
Supplementary Figure 5 | Specific heat data for the flux-core-free solder (Sn45-Pb55). **a,b**, Squared temperature (T^2) dependence of the specific heat (C) in a form of C/T measured at $H = 0$ Oe for the flux-core-free Sn45-Pb55 solder. The data were taken after zero-field cooling (ZFC) and field cooling at $H = 1500$ Oe (FC). In **Supplementary Figure 1b**, clear differences appear below transition temperature (T_c) of Sn. **c**, T^2 dependence of C/T measured at $H = 1500$ Oe for Sn45-Pb55. **d**, Low-temperature analysis for the data $H = 1500$ Oe where C/T was fitted using a formula of $C/T = \gamma + \beta T^2 + \delta T^4$. Debye temperature (θ_D) was calculated as $128.8(4) \text{ K}$ using β and the relation of $\beta = 12\pi^4 N k_B / \theta_D^3$ where N and k_B are the number of atoms and Boltzmann constant, respectively.



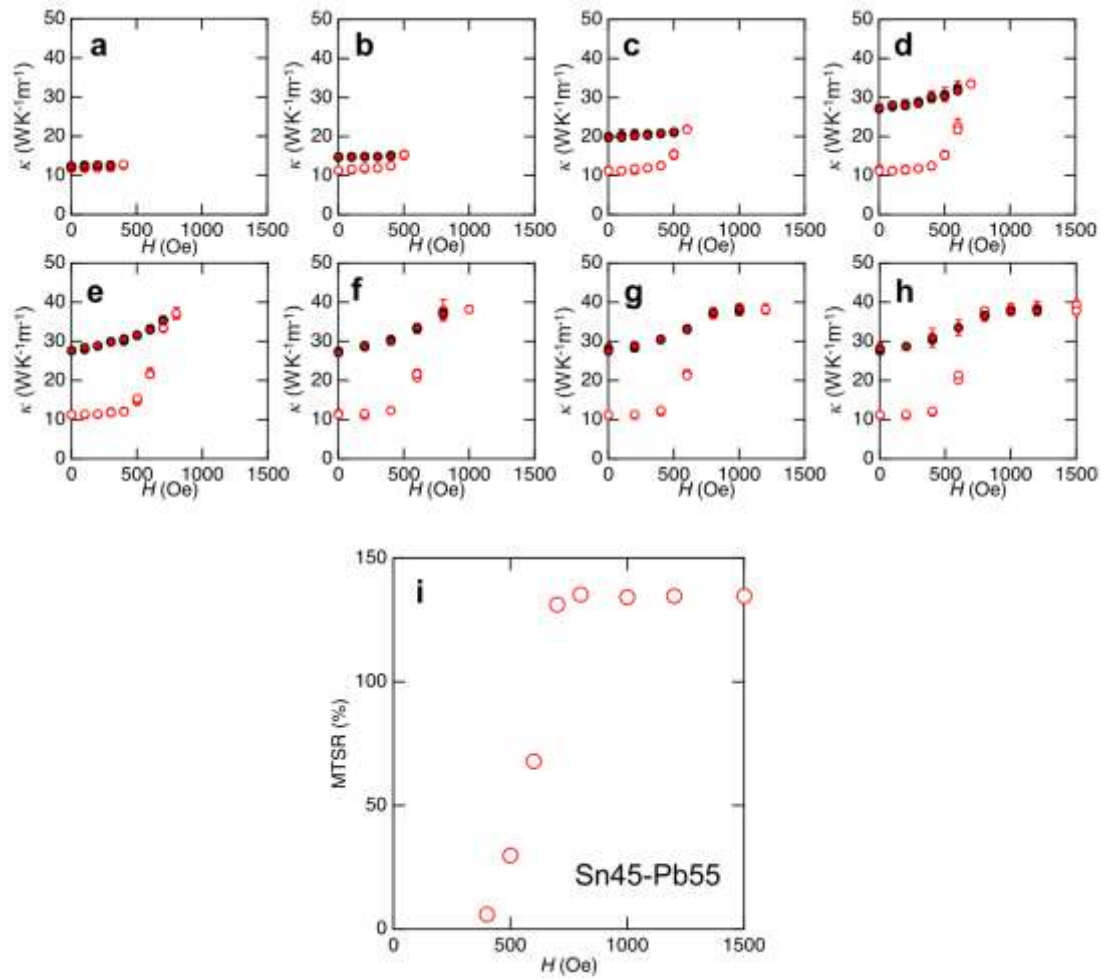
Supplementary Figure 6 | Stability of the trapped flux. Time dependence of magnetization for flux-core-free Sn45-Pb55 solder measured at $T = 2.5$ K for 40 h.



Supplementary Figure 7 | Magneto-optical (MO) imaging. We performed MO imaging on the Sn₄₅-Pb₅₅ solder at $T = 2.5$ K after different magnetic-field experiences. The bubble-like particles on all images are extrinsic impurities on the microscope system. Light parts correspond to positive magnetic fluxes. Image (i) is taken after ZFC, and no magnetic fluxes are observed. Image (ii) and (iv) are taken at $H = 1500$ and -1500 Oe, respectively; μm -order structures, which indicate the uniform presence of magnetic fluxes in the normal conducting states, are observed. Image (iii) and (v) are taken at $H = 0$ Oe but with positive and negative flux trapping, respectively. Here, similar structures observed in image (ii) and (iv) are present, but they are blurred. The blurriness would be caused by the presence of inhomogeneity of Sn/Pb regions along the thickness direction because of the sample thickness of about 100 μm . The noticeable features are the appearance of different contrast between (ii) and (iii) and between (iv) and (v). The dark parts in image (iii) and light parts in image (v) correspond to the Pb-rich regions in the Meissner states.



Supplementary Figure 8 | Tunable nonvolatile MTSR by Sn-Pb composition. **a,b**, Temperature dependence and field dependence of κ for the Sn10-Pb90 solder wire. **c,d**, Temperature dependence and field dependence of κ for the Sn90-Pb10 solder wire. **e,f**, SEM-EDX analyses results for the Sn10-Pb90 and Sn90-Pb10 solders. MTSR denotes magneto thermal switching ratio.



Supplementary Figure 9 | Tunability of the ON value by tuning applied magnetic field. a–h, Field dependence of κ for the Sn45-Pb55 solder with different minor loops. **i**, Maximum field dependence of MTSR.